Materials Characterization 138 (2018) 107–112

Contents lists available at ScienceDirect

Materials Characterization

journal homepage: www.elsevier.com/locate/matchar

Structure and crystallography of martensite–austenite constituent in the intercritically reheated coarse-grained heat affected zone of a high strength pipeline steel

Xueda Li[a,*], Chengjia Shang[b,*], Xiaoping Ma[c], S.V. Subramanian[c], R.D.K. Misra[d], Jianbo Sun[a]

[a] College of Mechanical and Electronic Engineering, China University of Petroleum (East China), Qingdao 266580, China
[b] School of Materials Science and Engineering, University of Science and Technology Beijing, Beijing 100083, China
[c] Department of Materials Science and Engineering, McMaster University, Hamilton L8S 4L8, Canada
[d] Department of Metallurgical, Materials and Biomedical Engineering, University of Texas at El Paso, El Paso, TX 79968, USA

ARTICLE INFO

Keywords:
Heat affected zone
Martensite-austenite constituent
Structure
Crystallography
Martensitic transformation

ABSTRACT

The structure and crystallography of martensite-austenite (M-A) constituent in the intercritically reheated coarse-grained heat affected zone (ICCGHAZ) of X100 (690 MPa) pipeline steel weld joint was studied via multi-scale characterization. The results suggested that majority of the necklace-type M-A constituent in the ICCGHAZ preferred to form lamellar lath structure, which primarily consisted of lath martensite (87%). Only small fraction of retained austenite (9%) was found between martensite laths. The retained austenite had K-S orientation relationship with its neighboring martensite: $(10\text{-}1)_M$ // $(11\text{-}1)_\gamma$ and $[111]_M$ // $[011]_\gamma$. Adjacent martensite laths within M-A constituent had large misorientation but no fixed crystallographic orientation relationship which implied that martensite laths may nucleate independently and encounter with each other during growth. M-A constituent and matrix microstructure belonged to different prior austenite grains. The martensite laths within the M-A constituent did not inherit the crystallographic orientation of the parent matrix during the intercritical reheating and subsequent cooling process of the second pass welding.

1. Introduction

In low carbon microalloyed steels, microstructure of the heat affected zone (HAZ) usually consists of upper bainite or granular bainite that has acceptable toughness [1,2]. Brittle martensite is unlikely to form because of low carbon equivalent. Thus, M-A constituent is the main factor responsible for deterioration of toughness in the HAZ, especially in the coarse-grained HAZ (CGHAZ) and intercritically reheated coarse-grained HAZ (ICCGHAZ) [3–7]. The influence of size, morphology, volume fraction and distribution of M-A constituent on the toughness has been extensively studied [4–11]. The M-A constituent can decrease the toughness of the HAZ by promoting both initiation and propagation of cleavage fracture [12–14]. Microcracks introduced by cracking of large M-A constituent or debonding of blocky M-A constituent from the matrix can act as crack nucleation site [5,12,13], and thereby promote the initiation of cleavage fracture. Near-connected or necklace-type M-A constituent along the grain boundaries can change the fracture mechanism from nucleation-controlled to propagation-controlled [14] which promoted the propagation of cleavage fracture.

A few studies on the structure of M-A constituent in the HAZ of microalloyed steels have been reported [15–18]. As the name implies, M-A constituent usually contains untempered martensite and retained austenite [19]. Both twinned martensite and lath martensite were observed in the M-A constituent depending on different alloy design [15–17]. An increased fraction of retained austenite and presence of twinned martensite in M-A constituent on the addition of Al content from 0.038% to 0.070% (wt%) in a high strength low alloy steel has been reported [17], where twinned martensite was more detrimental to toughness [18]. Lambert et al. reported that austenite was distributed at the periphery, while martensite was at the center of M-A constituent in the simulated ICCGHAZ of a HSLA steel weld [16]. The difference in the structure of M-A constituent was a consequence of different alloying content and processing conditions (welding thermal cycles).

However, crystallography of M-A constituent in the HAZ has not been studied in detail to the best of our understanding. Study on the crystallographic relationship between martensite and retained austenite is expected to facilitate understanding the transformation mechanism of M-A constituent. This would help us optimize or control the M-A constituent and improve the HAZ toughness from the perspective of design of welding parameters. In the study described here, the structure and

* Corresponding authors.
E-mail addresses: xli@upc.edu.cn (X. Li), cjshang@ustb.edu.cn (C. Shang).

https://doi.org/10.1016/j.matchar.2018.01.042
Received 26 October 2017; Received in revised form 22 January 2018; Accepted 29 January 2018
Available online 05 February 2018
1044-5803/

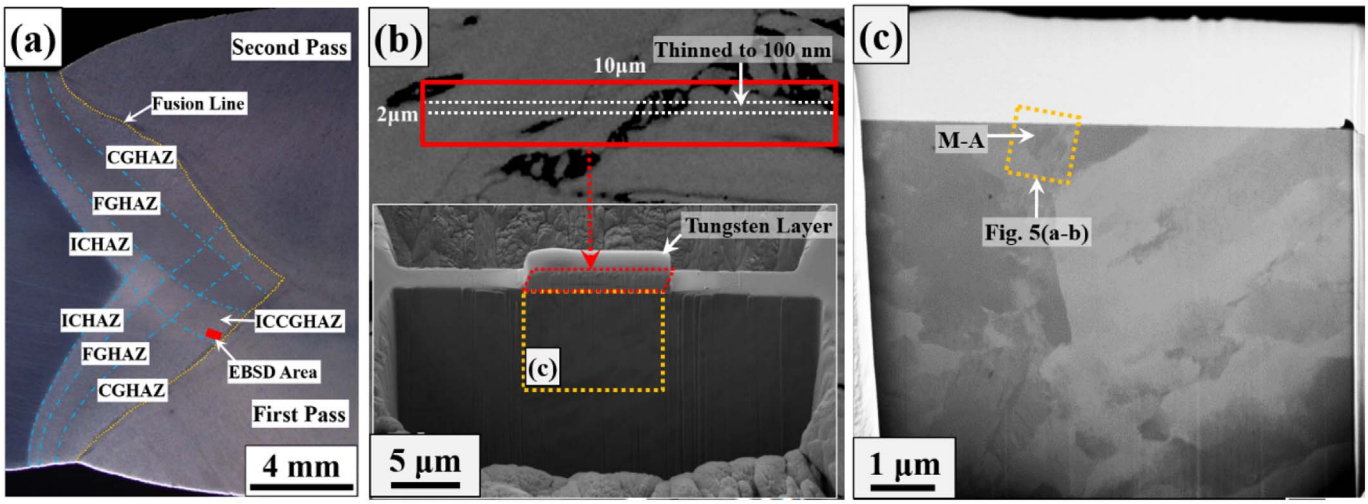

Fig. 1. (a) Macrograph of the weld joint, (b) schematic showing how the in-situ M-A particle was cut via FIB, and (c) SEM image of the FIB-milled TEM sample after thinning. (For interpretation of the references to color in this figure, the reader is referred to the web version of this article.)

crystallography of M-A constituent in the ICCGHAZ of a high strength (X100) pipeline steel weld joint was studied by means of multi-scale characterization, and transformation mechanism of M-A constituent in the ICCGHAZ was discussed.

2. Materials and Methods

The chemical composition (wt%) of X100 pipeline steel was Fe–0.07C–0.25Si–1.94Mn–0.081Nb–0.28Cr–0.26Mo–0.014Ti. A plate with thickness of 14.7 mm was made into pipe of ~1219 mm outer diameter. Dual pass submerged arc welding (SAW) was applied, and the heat input of each pass was 30 kJ/cm. The weld joint was cut from the as-welded pipe for the experimental study, and the macrograph of the weld joint is presented in Fig. 1a. Several sub-zones, i.e. CGHAZ, fine-grained HAZ (FGHAZ), intercritically reheated HAZ (ICHAZ), ICCGHAZ, etc. were formed because of the heat-affect of welding passes. Microstructure of the ICCGHAZ and structure of M-A constituent in the ICCGHAZ were characterized using optical microscope (OM, Zeiss Axio Plan), scanning electron microscope (SEM, JEOL JSM7000F), and transmission electron microscopy (TEM, Philips CM12). LePera etchant was used to determine the distribution of M-A constituent [20]. High resolution electron backscattered diffraction technique (EBSD, Oxford Synergy System) with 50 nm step size was used to detect the crystal structure of M-A constituent in the ICCGHAZ. Both BCC and FCC databases were added during the calibration of electron backscattered diffraction patterns (EBSPs).

In order to study the crystallographic relationship between the laths within the M-A constituent, one M-A particle was cut in-situ from the EBSD sample using focused ion beam (FIB) technique, as schematically presented in Fig. 1b. Prior to FIB milling, 2 × 10 μm (red square in Fig. 1b) and 1.5 μm thick tungsten layer was deposited to protect the surface from the damage of ion beam. As shown in Fig. 1b, the cutting plane (yellow dashed rectangle) was vertical to the EBSD scanning plane, and the cutting direction (white dashed line) was vertical to the laths within the M-A particle. Then, the sample was thinned to 100 nm thick using FIB (Fig. 1c), for observation via TEM. Bright/dark field images and diffraction patterns of the FIB-milled sample were obtained using FEI Titan 80-300LB TEM. The system could automatically obtain diffraction patterns dot-by-dot like 'diffraction scanning'. Diameter of the beam was 3 nm, and the step size was set as 30 nm. The sample was not rotated during 'scanning'. The obtained diffraction patterns were programmed to be calibrated automatically and the phase map of the 'scanned' area was reconstructed [21].

3. Results and Discussion

The X100 pipeline steel had a ferrite–bainite dual phase microstructure. After dual pass SAW welding, several HAZs were formed. The microstructure of CGHAZ consisted of coarse-grained (~80 μm) degenerated upper bainite [22] and granular bainite. FGHAZ was composed of fine-grained (~10 μm) polygonal ferrite and scattered bainite/M-A constituent. In ICHAZ, small fraction of scattered M-A constituent was formed at the interface of ferrite–bainite in the base metal. Detailed microstructure characterizations and structure-property relationship of X100 base metal and corresponding HAZs are reported in Ref. [2].

The microstructure characterization of the ICCGHAZ and M-A constituent is presented in Fig. 2. Similar to the CGHAZ, the matrix microstructure of the ICCGHAZ also consisted of degenerated upper bainite and granular bainite (Fig. 2a), and its average prior austenite grain size was ~80 μm. However, near-connected or continuously distributed M-A constituent (referred as necklace-type M-A constituent in [2,9,10]) was formed along the prior austenite grain boundaries. The distribution of M-A constituent in the ICCGHAZ was outlined using LePera etchant, as presented in Fig. 2b. The results showed that majority of the grain boundaries were decorated by necklace-type M-A constituent, and the area fraction of M-A constituent in the ICCGHAZ was calculated to be 3.7%. From the morphological aspect, M-A constituent along the prior austenite grain boundaries were mostly blocky-type, and those distributed between upper bainite laths were slender-type (Fig. 2c–d), according to the definition in Ref. [8]. Lamellar lath structure was frequently observed within the M-A constituent in the ICCGHAZ (Fig. 2d). TEM observations presented in Fig. 3 indicated that both blocky-type and slender-type M-A constituent preferred to form lath structure. Dark field TEM images (Fig. 3b and d) indicated that the adjacent laths may have large crystallographic misorientation.

High resolution EBSD technique was used to identify the crystal structure of the M-A constituent in the ICCGHAZ, and the results are presented in Fig. 4. Fig. 4a–b are band contrast maps in which BCC structure has gray color and FCC has red color. Very small fraction of FCC (austenite) phase was detected, as presented in Fig. 4a. Fig. 4b is the enlarged image of selected area in Fig. 4a, which contains 2 typical M-A particles. The M-A constituent had lamellar lath structure in which only BCC structure was identified. The sandwiched laths between the detected BCC structures were unindexed (black dots), which indicated that these regions had large residual stress and lattice distortion. Under this condition, the calibrating accuracy of the EBSPs was very low. The residual stress may come from phase transformation of M-A constituent or welding residual stress [23].